Dual-core photonic crystal fibers for tunable polarization mode dispersion compensation

D. C. Zografopoulos,[1,3] C. Vázquez,[1,4] E. E. Kriezis,[2,5] and T. V. Yioultsis[2,6]

[1] *Displays and Photonics Applications Group, Electronics Technology Department, Carlos III University of Madrid, 28911 Leganés, Madrid, Spain*

[2] *Department of Electrical and Computer Engineering, Aristotle University of Thessaloniki, Thessaloniki GR-54124, Greece*

[3] *dzografo@ing.uc3m.es*

[4] *cvazquez@ing.uc3m.es*

[5] *mkriezis@auth.gr*

[6] *traianos@auth.gr*

Abstract: A novel type of dual concentric core photonic crystal fiber (PCF) is proposed and theoretically analyzed, aiming at the design of tunable dispersive fiber elements for polarization-mode-dispersion (PMD) compensation. The adjustment of the fiber's geometrical birefringence through the proper selection of structural parameters leads to very high values of differential group-delay (DGD). Moreover, the value of DGD can be dynamically tuned by infiltrating the outer core capillaries of the PCF with an optical liquid, which allows for the thermal control of its refractive index. Such fibers are envisaged as tunable dispersive fiber elements for PMD compensation or emulation modules.

OCIS codes: (060.5295) Photonic crystal fibers; (060.2340) Fiber optics components; (230.2035) Dispersion compensation devices; (060.2420) Fibers, polarization-maintaining.

References and links

1. P. St. J. Russell, "Photonic-crystal fibers," J. Lightwave Technol. **24**, 4729–4749 (2006).
2. P. J. Roberts, B. J. Mangan, H. Sabert, F. Couny, T. A. Birks, J. C. Knight, and P. St. J. Russell, "Control of dispersion in photonic crystal fibers," J. Opt. Fiber. Commun. Rep. **2**, 435–461 (2005).
3. X. Zhao, G. Zhou, S. Li, Z. Liu, D. Wei, Z. Hou, and L. Hou, "Photonic crystal fiber for dispersion compensation," Appl. Opt. **47**, 5190–5196 (2008).
4. K. Thyagarajan, R. K. Varshney, P. Palai, A. K. Ghatak, and I. C. Goyal, "A novel design of a dispersion compensating fiber," IEEE Photon. Technol. Lett. **8**, 1510–1512 (1996).
5. F. Gérôme, J.-L. Auguste, J. Maury, J.-M. Blondy, and J. Marcou, "Theoretical and experimental analysis of a chromatic dispersion compensating module using a dual concentric core fiber," IEEE J. Lightwave Technol. **24**, 442–448 (2006).
6. A. Huttunen and P. Törmä, "Optimization of dual-core and microstructure fiber geometries for dispersion compensation and large mode area," Opt. Express **13**, 627–635 (2005).
7. T. Fujisawa, K. Saitoh, K. Wada, and M. Koshiba, "Chromatic dispersion profile optimization of dual-concentric-core photonic crystal fibers for broadband dispersion compensation," Opt. Express **14**, 893–900 (2006).
8. D. C. Zografopoulos and E. E. Kriezis, "Tunable optical fiber polarization elements based on long-period gratings inscribed in birefringent microstructured fibers," J. Opt. Soc. Am. B **25**, 111–118 (2008).

#149573 - $15.00 USD Received 20 Jun 2011; revised 16 Sep 2011; accepted 19 Sep 2011; published 19 Oct 2011

9. C.-P. Yu, J.-H. Liou, S.-S. Huang, and H.-C. Chang, "Tunable dual-core liquid-filled photonic crystal fibers for dispersion compensation," Opt. Express **16**, 4443–4451 (2008).
10. R. DeSalvo, A. G. Wilson, J. Rollman, D. F. Schneider, L. M. Lunardi, S. Lumish, N. Agrawal, A. H. Steinbach, W. Baun, T. Wall, R. Ben-Michael, M. A. Itzler, A. Fejzuli, R. A. Chipman, G. T. Kiehne, and K. M. Kissa, "Advanced components and sub-system solutions for 40Gb/s transmission," J. Lightwave Technol. **20**, 2154–2181 (2002).
11. A. Teixeira, L. Costa, G. Franzl, S. Azodolmolky, I. Tomkos, K. Vlachos, S. Zsigmond, T. Cinkler, G. Tosi-Beleffi, P. Gravey, T. Loukina, J. A. Lázaro, C. Vazquez, J. Montalvo, and E. Le Rouzic, "An integrated view on monitoring and compensation for dynamic optical networks: from management to physical layer," Photon. Netw. Commun. **18**, 191–210 (2009).
12. H. Bülow and S. Lanne, "PMD compensation techniques," J. Opt. Fiber Commun. Rep. **1**, 283–303 (2004).
13. X. Zhang, Y. Xia, Y. Huang, and X. Ren, "A novel tunable PMD compensation using linearly chirped fiber Bragg gratings," Opt. Commun. **214**, 123–127 (2002).
14. L. Yan, M. C. Hauer, Y. Shi, X. S. Yao, P. Ebrahimi, Y. Wang, A. E. Willner, and W. L. Kath, "Polarization-mode-dispersion emulator using variable differential-group-delay (DGD) elements and its use for experimental importance sampling," J. Lightwave Technol. **22**, 1051–1058 (2004).
15. N. M. Litchinitser, M. Sumetsky, and P. S. Westbrook, "Fiber-based tunable dispersion compensation," J. Opt. Fiber Commun. Rep. **4**, 41–85 (2007).
16. A. Pitilakis, D. C. Zografopoulos, and E. E. Kriezis, "In-line polarization controller based on liquid-crystal photonic crystal fibers," J. Lightwave Technol. **29**, 2560–2569 (2011).
17. Y. Huang, Y. Xu, and A. Yariv, "Fabrication of functional microstructured optical fibers through a selective-filling technique," Appl. Phys. Lett. **85**, 5182–5184 (2004).
18. K. Nielsen, D. Noordegraaf, T. Sörensen, A. Bjarklev, and T. P. Hansen, "Selective filling of photonic crystal fibres," J. Opt. A: Pure Appl. Opt. **7**, L13–L20 (2005).
19. J. Du, Y. Liu, Z. Wang, Q. Shi, Z. Liu, Q. Fang, J. Li, G. Kai, and X. Dong, "Two accesses to achieve air-core's selective filling of a photonic bandgap fiber," Proc. of SPIE **6781**, 678111 (2007).
20. J. Ju, H. F. Xuan, W. Jin, S. Liu, and H. L. Ho, "Selective opening of airholes in photonic crystal fiber," Opt. Lett. **35**, 3886–3888 (2010).
21. T. P. White, B. T. Kuhlmey, R. C. McPhedran, D. Maystre, G. Renversez, C. Martijn de Sterke, and L. C. Botten, "Multipole method for microstructured optical fibers. I. Formulation," J. Opt. Soc. Am. B **19**, 2322–2330 (2002).
22. B. T. Kuhlmey, T. P. White, G. Renversez, D. Maystre, L. C. Botten, C. Martijn de Sterke, and R. C. McPhedran, "Multipole method for microstructured optical fibers. II. Implementation and results," J. Opt. Soc. Am. B **19**, 2331–2340 (2002).
23. Cargille Labs, AAA series of refractive index liquids, `http://www.cargille.com`.
24. T. R. Woliński, P. Lesiak, K. Szaniawska, A. W. Domański, and J. Wójcik, "Polarization mode dispersion in birefringent microstructured fibers," Opt. Appl. **34**, 541–549 (2004).
25. W. Wadsworth, A. Witkowska, S. Leon-Saval, and T. Birks, "Hole inflation and tapering of stock photonic crystal fibers," Opt. Express **13**, 6541–6549 (2005).
26. Fibercore Ltd., FiberCore SM600 & SM1500, `http://www.fibercore.com`.
27. B. J. Eggleton, A. Ahuja, P. S. Westbrook, J. A. Rogers, P. Kuo, T. N. Nielsen, and B. Mikkelsen, "Integrated tunable fiber gratings for dispersion management in high-bit rate systems," J. Lightwave Technol. **18**, 1418–1420 (2000).
28. Q. Yu and A. W. Willner, "Performance limits of first-order PMD compensators using fixed and variable DGD elements," IEEE Photon. Technol. Lett. **14**, 304–306 (2002).
29. J. Du, Y. Liu, Z. Wang, B. Zou, B. Liu, and X. Dong, "Electrically tunable Sagnac filter based on a photonic bandgap fiber with liquid crystal infused," Opt. Lett. **33**, 2215–2217 (2008).

1. Introduction

Photonic crystal fibers (PCFs) constitute a special class of optical fibers, which are characterized by a cladding of air capillaries most commonly arranged in a triangular lattice. The form of the central defect core is associated with the PCF's light guiding mechanism: index-guiding in the case of a solid core, or bandgap-guiding when low-index or hollow cores are used. PCFs have been thoroughly investigated in the last years, since they offer extensive design capabilities, which allow for the tailoring of key-optical fiber properties, such as dispersion, non-linearity and birefringence [1].

Among these possibilities, efficient dispersion management has been shown by proper design of index-guiding silica PCFs. Control of the zero-dispersion wavelength, ultra-flattened dispersion, and chromatic dispersion optimized fiber structures have been widely studied and

#149573 - $15.00 USD Received 20 Jun 2011; revised 16 Sep 2011; accepted 19 Sep 2011; published 19 Oct 2011

demonstrated [2]. In particular, dual-concentric-core PCFs, formed by raising the refractive index of one of the cladding's rings, are characterized by very high absolute values of the chromatic dispersion (CD) coefficient D [3]. As in the case of their conventional counterparts [4, 5], dual-core PCFs support two supermodes whose anti-crossing at a specific wavelength may readily provide values of D in the range of thousands of ps/nm·km, allowing for efficient chromatic dispersion compensation [6]. The refractive index profile in the cladding of dual-core PCFs can be controlled by suitable selection of the air-capillaries dimensions, avoiding the need for doping, while permitting at the same time optimized slope-matching for CD compensation [7]. Moreover, PCFs offer the possibility of designing in-fiber elements with thermally tunable dispersive properties, by infiltrating all or some of its capillaries with an optical liquid [8, 9].

This work focuses on the design and study of a novel type of highly-birefringent dual-core PCFs. First, it is demonstrated that by appropriate adjustment of the structural and material parameters, the geometrically induced birefringence may result in very high values of differential group delay (DGD) within the spectral range of optical fiber communications windows. Next, a parametric study is performed focusing on the impact of various structural and material parameters on the DGD profile of the proposed PCFs. Finally, the possibility to thermally control the values of DGD is assessed, in the context of designing more functional tunable devices. Indeed, owing to the stochastic nature of PMD variations in high bit-rate fiber communication links [10, 11] and the increasing demand on techniques that allow dynamic compensation of impairments in order to provide reliable network performance, dispersive elements with tunable DGD are essential in the design of PMD compensating modules [12]. Contrary to existing tunable PMD compensation techniques, based on linearly chirped highly-birefringent fiber Bragg gratings [13], the PCFs here presented offer an in-fiber alternative solution, which covers a broad range of DGD values, while exhibiting also extensive thermal tunability. The proposed dispersive elements could also be exploited in PMD emulators, where controllable high-values of DGD are required in order to estimate the PMD-caused signal impairment in real long-haul optical fiber links [14], or to compensate the DGD induced by other components, such as fiber grating-based tunable chromatic dispersion compensation modules [15].

2. Tunable differential-group-delay in birefringent dual-core PCFs

2.1. Structural parameters

The layout of the proposed PCF is shown in Fig. 1(a). The fiberglass material is silica and the lattice of air-capillaries is characterized by a pitch Λ and a hole radius r. The air-hole radius r_d of one ring is reduced and its capillaries are infiltrated with a liquid of index n_d, so that the outer high-index core of the dual-core PCF is formed. The progressive coupling of optical power between the inner and the outer core leads to a notch in the dispersion curve of the supermodes supported by the fiber, which is responsible for the exceptionally high absolute values of D and, as it will be shown, those of DGD in the case of highly-birefringent PCFs. Selective infiltration of either the smaller or larger air-holes of a PCF's cladding can be readily achieved, for instance by exploiting the difference in the infusion length among capillaries of different radii [17, 18, 19, 20]. The radius r_1 of two air-holes adjacent to the fiber's inner core is modified, in order to induce geometrical birefringence. In addition, the radius r_6 of the last ring may be modified so as to control the level of confinement losses. The index of the infiltrated liquid can be thermally tuned, providing a means of dynamic control of the PCF's dispersive properties and, most important, the value of the induced DGD. As the key-element of a PMD-compensation module, the proposed dual-core PCF can provide the necessary compensating values of DGD, which in real long-haul systems are time-variant and follow a Maxwellian distribution [12]. Figure 1(b) shows the basic scheme and the components of an all-fiber PMD-compensation module, where the signal quality control feedback circuit drives a polarization

#149573 - $15.00 USD Received 20 Jun 2011; revised 16 Sep 2011; accepted 19 Sep 2011; published 19 Oct 2011

controller, also possibly PCF-based [16], and the proposed tunable-DGD dual-core PCF.

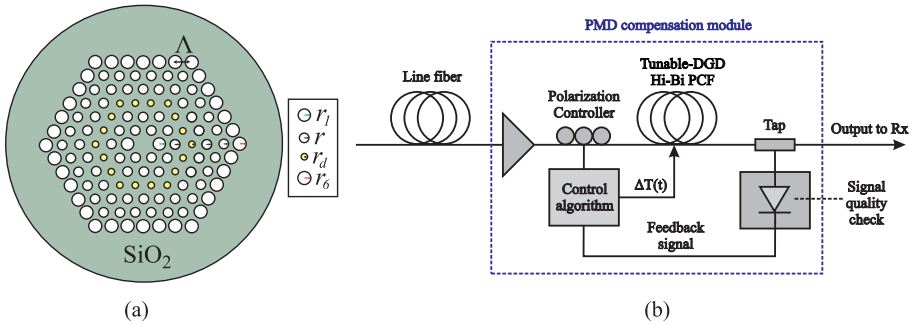

Fig. 1. (a) Layout of the proposed birefringent dual-core PCF. The lattice pitch equals Λ and the air-hole radius is r. The hole radius r_d of one ring is reduced in order to form the outer high-index fiber core. To induce birefringence, the radius r_1 of two air-holes adjacent to the fiber core is modified, as well as that of the last ring r_6 in order to control the level of confinement losses. The high-index ring capillaries are infiltrated with a liquid with refractive index n_d. (b) Basic scheme of a PMD compensation module composed of a polarization controller, the proposed PCF and a signal quality control feedback circuit.

2.2. Dispersion properties of dual-concentric-core PCFs

The PCF's modal dispersive properties are studied by means of the multipole method, which is capable of solving for the effective modal indices of the supermodes supported by the fiber [21, 22]. Material dispersion of silica is taken into account via the corresponding Sellmeier equation. As an initial indicative example, Fig. 2 shows the wavelength dependence of the CD coefficient $D(\lambda)$, when the third ring is infiltrated, for the following set of structural and material parameters, $\Lambda = 2.3\mu$m, $r = r_1 = r_6 = 0.65\mu$m, $r_d = 0.45\mu$m, and for three values of the liquid's index centered at $n_d = 1.33$. It is demonstrated that the minimum D wavelength can be tuned [9] with an efficiency of $0.64\text{nm}/10^{-4}\text{RIU}$. In the case of a typical optical liquid with a thermo-optic coefficient of $-3.34 \times 10^{-4}\text{RIU}/^{\circ}\text{C}$ [23], this translates to a thermal tuning efficiency of $2.14\text{nm}/^{\circ}\text{C}$. The modal intensity profiles at 1.5 and 1.6μm are shown in the inset for $n_d = 1.33$. At low wavelengths the optical power is confined in the inner core, while it progressively couples to the outer core towards longer wavelengths. The fundamental supermode's dispersion curve experiences a transition between the two modal curves of the isolated cores, whose anti-crossing leads to a notch in $D(\lambda)$ and to very high absolute values.

2.3. Differential group delay in highly-birefringent dual-concentric PCFs

Geometrical birefringence can be induced in the PCF structure by modifying the radius of the two air-holes adjacent to the fiber's core. Since this modification affects the geometry mostly of the central core, the fiber's polarization-dependent dispersive properties are expected to be altered mainly in the wavelength window where the fundamental supermode is confined in the inner core. Contrarily, the impact on the birefringence of the infiltrated outer core should be minimal.

Figure 3(a,b) shows the dispersion curves for the *x*- and *y*-polarized fundamental supermode, that is the one of the highest modal index, for a set of indicative examples and the corresponding modal birefringence B, defined as the difference between the indices n_y and n_x of the *y*- and *x*-polarized supermodes, respectively. Two individual cases are considered, assuming that the fiber's outer core is formed in the third (PCF A) or the fourth (PCF B) air-hole ring of the mi-

#149573 - $15.00 USD Received 20 Jun 2011; revised 16 Sep 2011; accepted 19 Sep 2011; published 19 Oct 2011

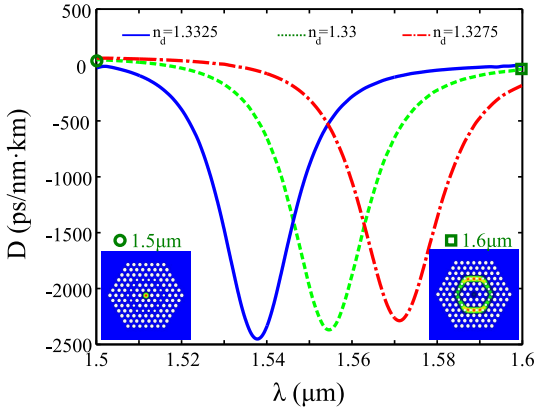

Fig. 2. Chromatic dispersion coefficient D of the dual-core PCF under study for $\Lambda = 2.3\mu$m, $r = r_1 = r_6 = 0.65\mu$m, $r_d = 0.45\mu$m, for three values of the infiltrated liquid's index. A tuning efficiency of the notch wavelength equal to $0.64\text{nm}/10^{-4}\text{RIU}$ is demonstrated. Inset shows the modal intensity profile of the fundamental supermode for $n_d = 1.33$ at 1.5μm (left) and 1.6μm (right).

crostructured cladding. Since the fundamental mode in the inner core is no longer degenerate, the dispersion curves of its two orthogonal polarizations split in the spectral window corresponding to wavelengths shorter than the two polarization-dependent notch wavelengths λ_x and λ_y, which in general depend on the fiber's structural parameters and the index of the infiltrated liquid n_d. For higher wavelengths both polarizations are confined in the symmetrical outer core and thus modal birefringence vanishes. In the region between λ_x and λ_y birefringence exhibits a drop, which is more abrupt when the outer-core is formed in the fourth rather than the third ring, as in that case the two cores are more optically isolated. The sign of B depends on r_1; for $r_1 > r$ it is shown that $n_y > n_x$, since in this case the $y-$polarized mode exhibits stronger confinement in the inner core, the opposite being the case for $r_1 < r$.

Apart from the fundamental mode, dual-core PCFs also support a second-order supermode, whose dispersive properties are in a sense reversed with respect to the fundamental one, that is optical power is confined in the inner (outer) core in the long (short) wavelength window, and its chromatic dispersion coefficient obtains the same absolute values, but with inverse sign [9]. In the case of the birefringent PCF here studied, these properties still apply separately for each polarization, as shown in Fig. 3(c). In the transition window between λ_x and λ_y, the slope of $B(\lambda)$ of the second-order supermode is positive and slightly larger in absolute value than that of the fundamental one, as the birefringence of the individual inner mode gradually rises with wavelength. Thus, since the second-order supermode is confined in the fiber's inner core in the wavelengths longer than the transition window, as shown in Fig. 3(d) where the modal intensity profiles for all modes are calculated at 1.55μm, its birefringence is larger compared to that of the fundamental one in the short-wavelength window.

It should be mentioned here that in all cases studied, when the fourth air-ring core is selected as the outer core r_6 is set equal to 0.95μm in order to reduce confinement losses, which are kept below 0.05dB/m for both polarizations in the entire wavelength window under study, and can be further reduced by adding more air-hole rings in the PCF's cladding. The maximum value reported corresponds to the long wavelength extreme of 1.7μm. Moreover, unless otherwise stated, the cladding hole radius is equal to $r = 0.65\mu$m, the outer core ring radius r_d is equal to 0.45μm and the pitch Λ is set to 2.3μm.

#149573 - $15.00 USD Received 20 Jun 2011; revised 16 Sep 2011; accepted 19 Sep 2011; published 19 Oct 2011

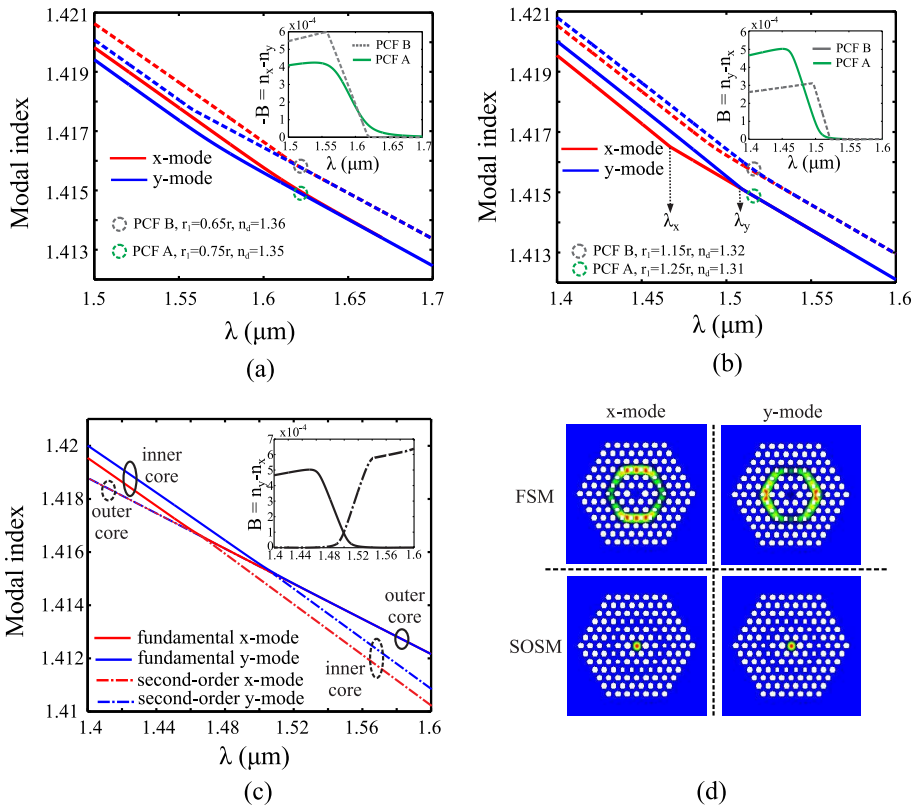

Fig. 3. Dispersion curves of the fundamental x- and y-polarized PCF supermode for a set of indicative cases ($\Lambda = 2.3\mu$m, $r = 0.65\mu$m, and $r_d = 0.45\mu$m) where (a) $r_1 < r$ and (b) $r_1 > r$ and for the outer core formed either in the third (PCF A) or the fourth (PCF B) ring of air-holes. Insets show the corresponding modal birefringence, which drops to zero when both polarizations are coupled in the outer ring. The transition is abrupt and linear in the case of the fourth-ring core, while it exhibits a more gradual profile when the third core is selected as the outer fiber core. (c) Dispersion curves and modal birefringence of both the fundamental and the second-order supermode for the example studied in (b), with the outer core formed in the third ring. (d) Modal intensity profiles for both supermodes and polarizations, calculated at 1.55μm. In the long wavelength window, the fundamental supermode (FSM) is confined in the outer ring-core, while the second order one (SOSM) in the inner core, exhibiting high values of birefringence.

The shape and particularly the slope of the wavelength-dependent birefringence $B(\lambda)$ influences directly the value of DGD, which depends on $B \equiv n_y - n_x$ according to

$$\mathrm{DGD} = \frac{1}{v_{g,y}} - \frac{1}{v_{g,x}} = \frac{1}{c}\left(B - \lambda \frac{dB}{d\lambda}\right), \tag{1}$$

$v_{g,i}$ being the polarization-dependent group velocity, and c the speed of light in vacuum. In typical conventional or photonic crystal polarization-maintaining fibers B is a smooth function of λ and the two terms in (1) are comparable, leading to values of DGD in the range of a few ps/m [24]. Nevertheless, in the case of the dual-core PCFs under study, owing to the high slope of B in the transition window between λ_x and λ_y, the second term in (1) dominates and leads to very high values of DGD. Figure 4 shows the DGD calculated for two sets of parameters

#149573 - $15.00 USD Received 20 Jun 2011; revised 16 Sep 2011; accepted 19 Sep 2011; published 19 Oct 2011

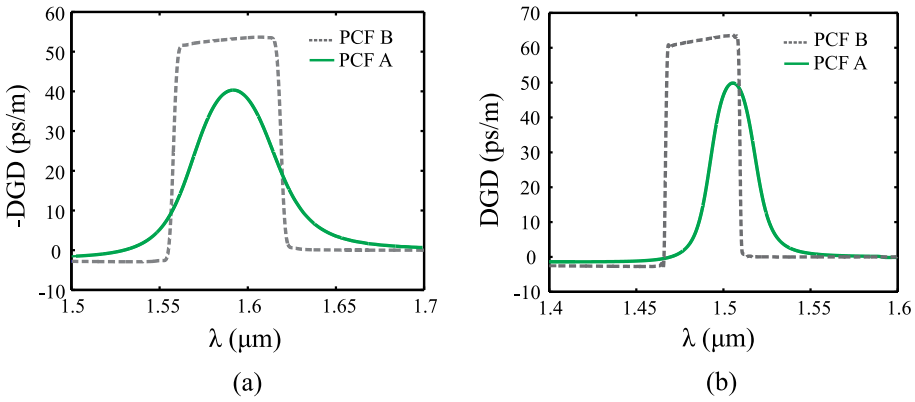

Fig. 4. Differential-group-delay of the proposed dual-core PCF for $\Lambda = 2.3\mu$m, $r_d = 0.45\mu$m and (a) $r_1 = 0.65r$, $n_d = 1.36$ and (b) $r_1 = 1.15r$, $n_d = 1.32$ (third-ring outer core), and $r_1 = 1.25r$, $n_d = 1.31$ (fourth-ring outer core). In the case of the fourth-ring DGD(λ) is almost piecewise-constant, obtaining high values in the window between the wavelength notches corresponding to the anti-crossing of the two polarizations of the fundamental mode, while in that of the third-ring DGD(λ) exhibits a Gaussian-like profile.

where either the third or the fourth ring is selected as the outer core. Far from the transition region between λ_x and λ_y the first term in (1), which is directly proportional to B, influences the total value of DGD. Within the transition window, DGD obtains values higher than 60ps/m and 50ps/m, when the outer core is placed in the fourth and third ring, respectively. When the fourth ring is selected as the outer core, the DGD spectral profile shows an abrupt rise and drop at λ_x and λ_y, and maintains an almost constant value in between. In the case of the third-ring outer core the DGD exhibits a smoother Gaussian-like profile. Such values of DGD indicate that PMD compensation of long-haul fiber links can be achieved by using a short piece of the proposed PCF [10]. Although the results here presented refer to the fundamental supermode, equally high values of DGD with opposite sign can be achieved for the second-order mode, since the slope of $B(\lambda)$ within the transition window is in that case positive, as shown in the inset in Fig. 3(c).

2.4. Effect of the PCF structural and material parameters on the values of DGD

In order to investigate into the dependence of DGD on modal birefringence we extended our study by letting r_1 vary in the interval $0.6r < r_1 < 1.4r$. A strong red- (blue-) shift is observed when r_1 is smaller (larger) than r. The DGD curves can be shifted back into the telecom window by properly adjusting the value of n_d as shown in Fig. 5(a), where the maximum DGD wavelength and the liquid index values used in the simulations are cited. The selection of these values of n_d, although not unique, ensures that the high-DGD profile of the proposed PCF covers approximately the same spectral windows for $r_1 > r$ and $r_1 < r$, so that results may be directly compared and thus the impact of B over DGD can be assessed. Although the wavelength where DGD is maximized does not coincide exactly among the cases studied, Figure 5(b) reveals that while an increase (decrease) of n_d leads to blue- (red-) shifting of DGD(λ), all other spectral characteristics of the DGD profile are not significantly affected. Given that, the impact of other key structural parameters can also be studied, as it will be demonstrated in the following of the performed analysis.

Figure 6(a) shows the dependence of the maximum value of DGD on the radius r_1, while the inset shows the corresponding peak value of B. The calculated values refer directly to the

#149573 - $15.00 USD Received 20 Jun 2011; revised 16 Sep 2011; accepted 19 Sep 2011; published 19 Oct 2011

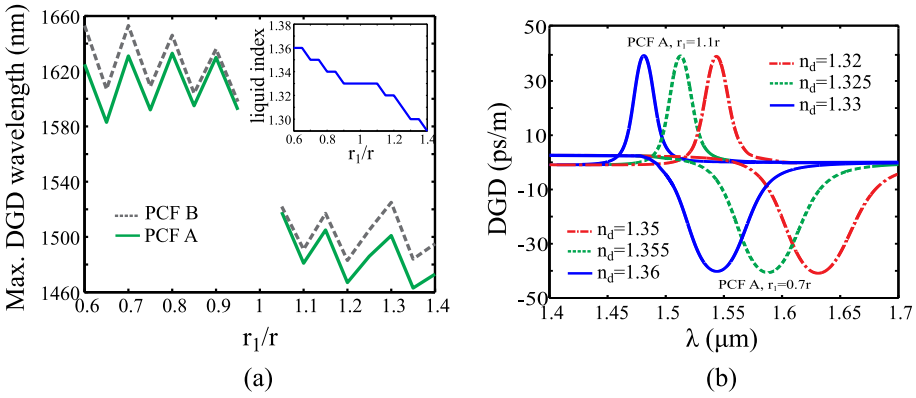

Fig. 5. (a) Wavelength of maximum calculated DGD and (inset) refractive index values of the infiltrated liquid used in the simulations. (b) DGD spectral profile for two indicative cases where the third ring is infiltrated for varying values of n_d. An increase of the liquid's refractive index leads to a blue-shift of DGD(λ), without affecting its other spectral characteristics.

results presented in Fig. 5(a), where the corresponding structural and material parameters, as well as the wavelengths where DGD is maximized are quoted. In the case of PCF A, the curve of $B = B(\lambda)$ shows a more gradual variation compared to that of PCF B, as the inner and outer core are less isolated, which facilitates optical power coupling between them. This leads to a less steep slope of B and, as a consequence, the maximum absolute value of DGD rises smoothly as r_1 deviates from r. On the other hand, in the case of PCF B, where the outer core is formed in the fourth ring, the transition between maximum and zero birefringence is abrupt and almost linear, which implies a constant value of $dB/d\lambda$. Thus, even for small deviations of r_1 almost the same maximum value of DGD is predicted as demonstrated in Figure 6(b), which shows the wavelength dependence of birefringence and the DGD profile for $r_1 = 1.05r$ and $r_1 = 1.3r$. It can be noticed that as the slope of $B(\lambda)$ is almost identical in both cases, the same also holds for the maximum DGD value. Nevertheless, as the transition window between λ_x and λ_y is larger in the case of larger r_1 the high-DGD window is also extended, up to more than 50nm for $r_1 = 1.3r$.

The spectral extent of the high-DGD window with respect to r_1 is thoroughly investigated in Fig. 7. It is shown that higher absolute values of modal birefringence, according to the inset of Fig. 6(a), raise the full-width at half-maximum (FWHM) of the DGD spectral profile, namely the window defined by the two λ where the value of DGD drops to half of its maximum value. This property might be of use in PMD-emulator systems, where large values of PMD may be induced in a broad wavelength band in order to assess the effect of PMD on the signal quality of WDM systems. In the context of assessing the tunability of the DGD value, a more important parameter is the the transition between zero and maximum level of DGD, which can be quantified via $\Delta\lambda^{\text{rise}} = \lambda^{90\%} - \lambda^{10\%}$, that is the increment defined by two wavelengths where DGD obtains 90% and 10% of its maximum value, respectively. The inset in Fig. 7 demonstrates that the transition is very abrupt in the case of the fourth-ring outer core, with $\Delta\lambda^{\text{rise}}$ obtaining very low values, less than 5nm. On the contrary, infiltration of the third core leads to smoother transitions, implying more efficient and controllable DGD-tuning. For this purpose, the rest of the results in the present study refer to the case of selecting the third ring as the fiber's outer core.

Since the outer core is essentially composed of two materials, silica and the infiltrated liquid

#149573 - $15.00 USD Received 20 Jun 2011; revised 16 Sep 2011; accepted 19 Sep 2011; published 19 Oct 2011

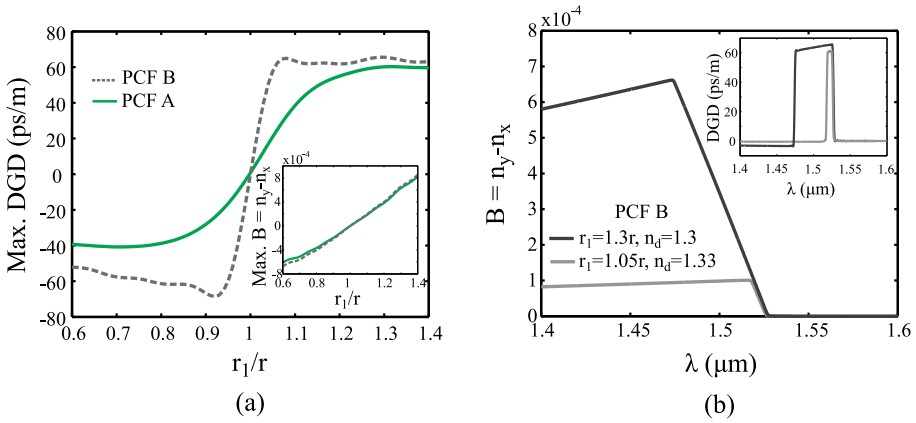

Fig. 6. (a) Maximum DGD and birefringence values for the dual-core PCF under study obtained for various values of r_1, with reference to the results shown in Fig. 5(a). DGD raises gradually with birefringence when the third ring is selected as the outer core. DGD values of up to 70 and 60 ps/m can be readily achieved for the outer core placed in the fourth and the third ring, respectively. (b) Modal birefringence and DGD profile when the fourth-ring is infiltrated for $r_1 = 1.3r$, $n_d = 1.3$ and $r_1 = 1.05r$, $n_d = 1.33$. As the slope of $B(\lambda)$ is almost equal in the two cases, the maximum DGD value is not significantly affected by the fiber birefringence maximum value.

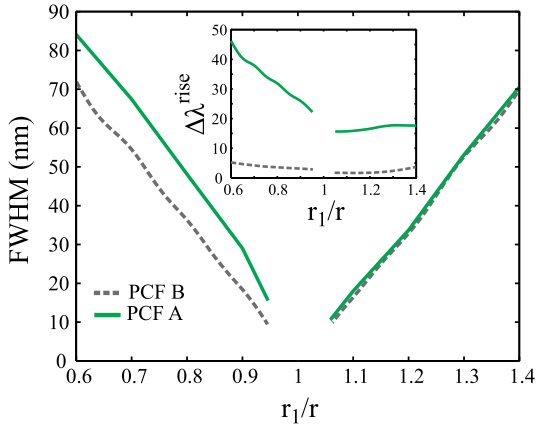

Fig. 7. Spectral extent (FWHM) of the high-DGD window and (inset) wavelength increment $\Delta\lambda^{\text{rise}}$, defined as the distance between wavelengths at which DGD obtains 10% and 90% of its maximum value, for the PCF under study. Very abrupt transitions are predicted when the outer core is placed in the fourth ring of the PCF's cladding.

in the capillaries, its effective index depends both on the radius r_d and the refractive index n_d of the optical liquid. Figure 8 studies the impact of the geometry and the material infiltrated in the outer core, for sets of parameters that maintain the high-DGD spectral profile within the C-band. It is shown that the increase of r_d and n_d leads to higher values of DGD, although in that case FWHM and $\Delta\lambda^{\text{rise}}$ decrease, indicating a more abrupt transition. Apart from providing higher DGD-values, larger radii r_d may also facilitate the infiltration process. For $r_d = 0.8\mu$m and $n_d = 1.404$ the maximum value of DGD exceeds 100ps/m at 1.54μm.

Figure 9 investigates the impact of the overall dimensions of the fiber, which are directly

#149573 - $15.00 USD Received 20 Jun 2011; revised 16 Sep 2011; accepted 19 Sep 2011; published 19 Oct 2011

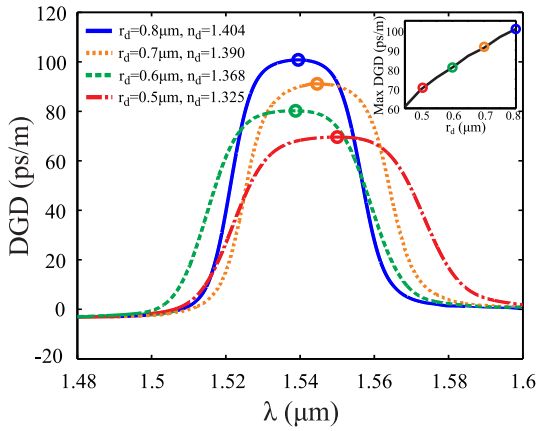

Fig. 8. DGD profiles for different values of the outer core radius and the index of the infiltrated liquid for $r_1 = 1.3r$. Higher values of DGD can be obtained by simultaneously raising r_d and n_d, for the same wavelength window. Inset shows the maximum obtainable values of DGD with respect to the infiltrated capillary radius r_d, for the set of cases studied.

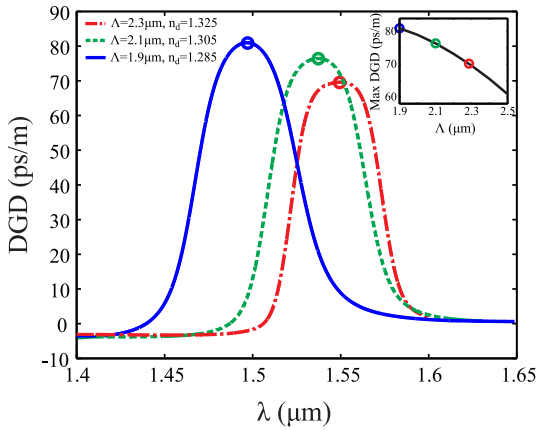

Fig. 9. DGD profiles for different values of the lattice pitch Λ, with relative structural parameters r/Λ and r_d/Λ kept the same. Smaller values of Λ blue-shift DGD(λ) and lead to higher DGD. The spectral position of DGD(λ) can be controlled by adjusting the liquid's index n_d. The inset shows the maximum DGD value obtained in the cases studied, for Λ ranging from 1.9 to 2.5μm.

related to the triangular lattice pitch Λ. Keeping the same value for the relative geometrical dimensions, namely $r_d = (0.5/2.3)\Lambda'$ and $r = (0.65/2.3)\Lambda'$, the pitch value is modified, along with n_d in order to shift the DGD profile in the same wavelength window. The increase of Λ red-shifts the DGD profile and lowers the maximum attainable DGD, as demonstrated in the inset. Although higher Λ provide lower DGD values, they enable coupling of the proposed fiber with other PCF or SMFs by raising the dimensions of the core and the modal field diameters. On the other hand, PCFs with small pitches provide larger values of DGD, implying that shorter fiber lengths may be required in PMD-control applications.

#149573 - $15.00 USD Received 20 Jun 2011; revised 16 Sep 2011; accepted 19 Sep 2011; published 19 Oct 2011

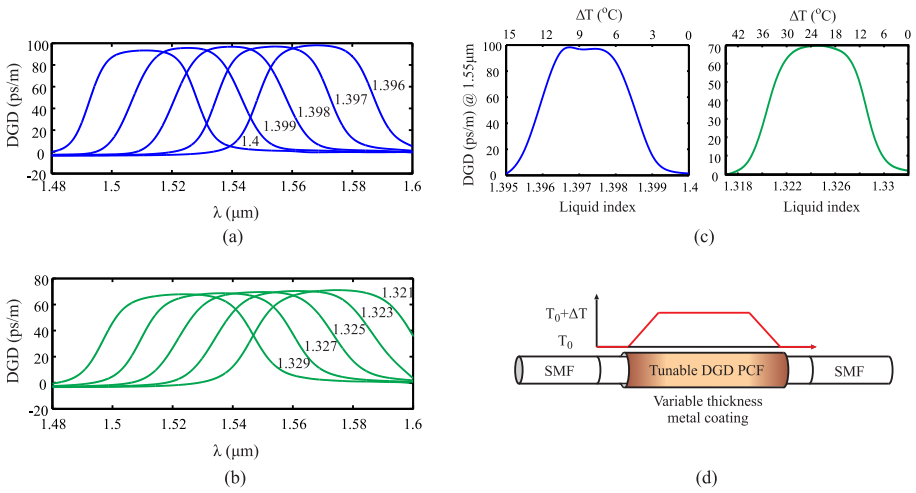

Fig. 10. DGD-tuning characteristics for two indicative cases of the proposed dual-core birefringent PCF. DGD curves with respect to the index n_d of the liquid infiltrating the third core for (a) $r_1 = 1.3r$, $r_d = 0.75\mu$m and (b) $r_1 = 1.3r$, $r_d = 0.5\mu$m. (c) The correspoding value of DGD at 1.55μm with respect to n_d or, equivalently, a temperature variation ΔT, assuming a thermo-optic coefficient of -3.34×10^{-4}RIU/°C. (d) A proposed layout for the efficient tuning of DGD in the proposed PCF: light is in- and out-coupled at ambient temperature where both polarizations are confined in the same core and it is gradually heated in order to induce the desired value of DGD.

2.5. *Thermal tuning of DGD in dual-core PCFs*

The analysis thus far has shown that the proposed dual-core birefringent PCFs provide exceptionally high values of DGD, owing to the intense slope of modal birefringence within the transition window related to the anti-crossing of the two orthogonal polarizations of the fundamental supermode. The spectral window, the bandwidth, the maximum DGD value and the rise wavelength increment depend on the structural and material parameters of the fiber, one of which is the refractive index n_d of the infiltrated material. Dynamic tuning of the DGD value is possible by thermally adjusting the value of n_d. Figure 10 investigates two indicative examples of the cases studied in terms of their tunability efficiency. The DGD spectral profiles for varying n_d is shown in Figs 10(a,b), where $r_1 = 1.3r$ and r_d is equal to 0.75μm and 0.5μm, respectively. The value of DGD at 1.55μm for both cases with respect to n_d is presented in Fig. 10(c), along with the corresponding temperature variations ΔT needed to induce the necessary Δn_d, assuming a thermo-optic coefficient of -3.34×10^{-4}RIU/°C for the optical liquid [23]. The case where $r_d = 0.75\mu$m shows enhanced thermal tunability, since the liquid occupies more space in the outer core. A total variation of 6°C and 18°C is needed in order to cover the full transition from zero to maximum DGD for the two examples, which in the case of a typical resolution of 0.1°C of temperature control stages, implies both adequate control of the exact DGD value and limited ΔT. Coupling of the proposed PCF to conventional SMFs depends on the structural parameters, as shown in Fig. 9, and can be optimized by using various PCF to SMF coupling techniques [25], or by selecting similar dimension commercially available SMFs [26].

A layout for the efficient control of the induced DGD in the dual-core PCFs under study is proposed in Fig. 10(d). A metal coating of variable thickness is placed around the fiber so that at the fiber input and output the temperature variation is very low owing to increased metal thickness and thus reduced current density [27]. The coating thickness is gradually reduced so

#149573 - $15.00 USD Received 20 Jun 2011; revised 16 Sep 2011; accepted 19 Sep 2011; published 19 Oct 2011

that in the main part of the fiber the desired temperature variation ΔT is induced. This configuration permits in- and out-coupling of light at ambient temperature, which can be selected by properly fixing n_d so that both polarization are confined in either one of the fiber cores, that is away from the transition window, as both the fundamental and the second-order supermodes are capable of providing comparably high values of DGD. In-between, the fiber is gradually heated in order to develop the modal profiles corresponding to the two polarizations, and thus induce the desired value of DGD. Since optical liquids are characterized by a negative thermo-optic coefficient [23], heating always results in a decrease of the liquid's refractive index. Assuming light coupling into the inner core is selected, as it presents significantly lower complexity, the proposed layout implies exciting the second-order mode at the long-wavelength edge of the transition window and heating of the fiber in order to tune the DGD value. In that case, the fundamental supermode is well confined in the outer core, as in the indicative case shown in Fig. 3(d), located at a radius of 3Λ, while the modal field radius (MFR) of the second-order supermode is comparable to Λ. Therefore, efficient selective excitation of the inner core mode is feasible by coupling light in the proposed PCF with a small-core SMF with similar MFR, such as, for instance, SM1500 by Fibercore [26]. For the particular case of Fig. 3(d), the calculation of the overlap integrals of the modal profiles of the dual-core PCF and that of SM1500 revealed for both polarizations an overlap coefficient higher than 80% for the second-order supermode, while less than 2% for the fundamental one, indicating that efficient coupling can be achieved. Other options include the use of a cooling rather than heating stage, so that the fundamental supermode at the short wavelength edge of the same window could be instead excited, as in that case it is confined in the inner core of the fiber.

In a more elaborate configuration, various pieces of the proposed PCF may be combined in a more efficient multi-stage layout, which allows for the compensation of higher-order PMD as well [28]. Finally, PCFs of this type might also be exploited in applications where variable birefringence is required, such as in tunable Sagnac optical filters [29].

3. Conclusions

The dispersive properties of dual-concentric-core birefringent PCFs have been investigated via a theoretical analysis based on the multipole method. It is shown that high values of differential group delay can be induced in such fibers, due to the abrupt slope of modal birefringence corresponding to the two polarizations of the fiber's supermodes. The value and spectral position of DGD can be adjusted by properly selecting the geometrical parameters of the PCF's structure. Thermal tuning is also possible by infiltrating the outer core's air-holes with an optical liquid with a high thermo-optic coefficient. Tunable DGD values up to 100ps/m are predicted for a thermal variation of 15°C. Such thermally tunable dispersive elements may be integrated in PMD compensation or emulation modules as an all-fiber solution that provides lower complexity and the same functionality in a wider wavelength window when compared to tension-tuned, chirped highly-birefringent fiber Bragg gratings, which constitute the main choice for fiber-based dynamic optical PMD compensation.

Acknowledgements

This work has been partially supported by the Research Committee of the Aristotle University of Thessaloniki, by the UC3M Talent Human Resources Contract, and by the Spanish Ministry of Science and Innovation within project TEC2009-14718-C03-03.

#149573 - $15.00 USD Received 20 Jun 2011; revised 16 Sep 2011; accepted 19 Sep 2011; published 19 Oct 2011